SIRPα polymorphisms, but not the prion protein, control phagocytosis of apoptotic cells

Mario Nuvolone,[1,2,3] Veronika Kana,[1] Gregor Hutter,[1] Daiji Sakata,[1] Steven M. Mortin-Toth,[4,5,6] Giancarlo Russo,[7] Jayne S. Danska,[4,5,6] and Adriano Aguzzi[1]

[1]Institute of Neuropathology, University Hospital of Zurich, CH-8091 Zurich, Switzerland
[2]Amyloidosis Research and Treatment Centre, Foundation IRCCS San Matteo Hospital; and [3]Department of Molecular Medicine, Institute for Advanced Studies; University of Pavia, 27100 Pavia, Italy
[4]Program in Genetics and Genome Biology, Hospital for Sick Children; [5]Department of Immunology; and [6]Department of Medical Biophysics; Faculty of Medicine, University of Toronto, Toronto, Ontario M5S 2J7, Canada
[7]Functional Genomics Center Zurich, CH-8057 Zurich, Switzerland

Prnp−/− mice lack the prion protein PrP[C] and are resistant to prion infections, but variable phenotypes have been reported in *Prnp*−/− mice and the physiological function of PrP[C] remains poorly understood. Here we examined a cell-autonomous phenotype, inhibition of macrophage phagocytosis of apoptotic cells, previously reported in *Prnp*−/− mice. Using formal genetic, genomic, and immunological analyses, we found that the regulation of phagocytosis previously ascribed to PrP[C] is instead controlled by a linked locus encoding the *signal regulatory protein α* (*Sirpa*). These findings indicate that control of phagocytosis was previously misattributed to the prion protein and illustrate the requirement for stringent approaches to eliminate confounding effects of flanking genes in studies modeling human disease in gene-targeted mice. The plethora of seemingly unrelated functions attributed to PrP[C] suggests that additional phenotypes reported in *Prnp*−/− mice may actually relate to *Sirpa* or other genetic confounders.

CORRESPONDENCE
Adriano Aguzzi:
adriano.aguzzi@usz.ch
OR
Jayne S. Danska:
jayne.danska@sickkids.ca

Abbreviations used: Chr 2, chromosome 2; ES, embryonic stem; gDNA, genomic DNA; pMΦ, peritoneal macrophage; RFLP, restriction fragment length polymorphism; SNP, single nucleotide polymorphism; STR, short tandem repeat.

The cellular prion protein PrP[C], encoded by the *Prnp* gene, is tethered to the membrane of most mammalian cells by a glycosylphosphatidylinositol anchor. Conversion and aggregation of PrP[C] into a misfolded conformer (termed PrP[Sc]) triggers transmissible spongiform encephalopathies, also termed prion diseases (Aguzzi and Calella, 2009). Disparate functions have been ascribed to PrP[C] on the basis of phenotypes described in *Prnp*−/− mice (Steele et al., 2007; Linden et al., 2008), yet none of these functions has been clarified mechanistically, and their validity was frequently challenged.

All currently available *Prnp*−/− lines were generated using embryonic stem (ES) cells derived from the 129 strain of *Mus musculus*. Typically, chimeric founder mice were crossed with WT (*Prnp*wt/wt) mice of the C57BL/6 strain (B6; Table 1). The resulting mice carrying the targeted allele were maintained as a mixed B6/129 background (B6129) or backcrossed to inbred strains (mainly B6), often for >10 generations, to generate congenic B6.129 mice (the period in B6.129

denotes congenesis, as opposed to mixed B6129 mice). Although the latter approach progressively reduces the contribution of the 129-derived genome, *Prnp*-linked genomic intervals may co-segregate with *Prnp* (Sparkes et al., 1986). Consequently, congenic *Prnp*wt/wt and *Prnp*−/− mice may differ at additional polymorphic loci (Smithies and Maeda, 1995; Gerlai, 1996). We hypothesized that co-segregation of linked genes may have confounded the attribution of functions to PrP[C] based on phenotypes observed in *Prnp*−/− mice (Collinge et al., 1994; Lledo et al., 1996; Walz et al., 1999; Rangel et al., 2007; Laurén et al., 2009; Calella et al., 2010; Gimbel et al., 2010; Ratté et al., 2011; Striebel et al., 2013).

Here we selected a cell-autonomous phenotype previously reported in congenic B6.129-*Prnp*ZrchI/ZrchI mice (Büeler et al., 1992): inhibition of phagocytosis of apoptotic cells (de Almeida et al., 2005). We used RNA sequencing to identify

M. Nuvolone, V. Kana, and G. Hutter contributed equally to this paper.

The Rockefeller University Press $30.00
J. Exp. Med. 2013 Vol. 210 No. 12   2539–2552
www.jem.org/cgi/doi/10.1084/jem.20131274

2539

Table 1. *Prnp* KO mouse lines analyzed in this study

Prnp KO mouse line	ES cells	Origin of ES cells	Strain of partner of chimeric mouse	Location of colony	Reference
Prnp^{ZrchI/ZrchI}	AB1	129S7/SvEvBrd	B6	Zurich, Switzerland	Büeler et al. (1992)
Prnp^{Ngsk/Ngsk}	J1	129S4/SvJae	B6	Nagasaki, Japan	Sakaguchi et al. (1995)
Prnp^{Edbg/Edbg}	E14	129/Ola	129/Ola	Edinburgh, Scotland, UK	Manson et al. (1994)
Prnp^{GFP/GFP}	HM-1	129/Ola	B6	Cambridge, MA	Heikenwalder et al. (2008)
Prnp^{Rkn/Rkn}	E14	129P2/OlaHsd	B6	Wako-shi, Japan	Yokoyama et al. (2001)
Prnp^{ZrchII/ZrchII}	E14.1	129/OlaHsd	B6	Zurich, Switzerland	Rossi et al. (2001)
Prnp^{Rcm0/Rcm0}	HM-1	129/Ola	129/Ola	Edinburgh, Scotland, UK	Moore et al. (1995)

The present study is based on the analysis of mice carrying seven independently generated *Prnp*-null alleles. *Prnp^{Edbg/Edbg}* and *Prnp^{Rcm0/Rcm0}* were always crossed to isogenic 129/Ola mice, whereas all other *Prnp^{−/−}* mice were crossed to B6 mice and then kept on a mixed B6 and 129 background or further backcrossed to B6 or other strains.

genes linked to *Prnp* and expressed in macrophages that may influence this phenotype. We report genetic and functional evidence that the regulation of phagocytosis previously ascribed to *Prnp^{−/−}* is instead controlled by the closely linked gene *signal regulatory protein α* (*Sirpa*; Matozaki et al., 2009).

RESULTS

RNA sequencing indicates *Sirpa* as a candidate modulator of phagocytosis

Because hyperphagocytosis was reported in *Prnp^{ZrchI/ZrchI}* mice after extensive backcrossing to B6, we reasoned that any genetic confounders leading to this phenotype in B6.129-*Prnp^{ZrchI/ZrchI}* mice would need to be physically linked to *Prnp*, polymorphic between 129 and B6 strains, and expressed in macrophages. To identify such genes, we performed RNA sequencing on B6.129-*Prnp^{ZrchI/ZrchI}* and B6.129-*Prnp^{wt/wt}* peritoneal macrophages (pMΦs). Of 11,586 genes, 305 were differentially expressed between the two groups (Fig. 1 A and Table S1). We then analyzed the reads for the presence of deviations from the B6 reference transcriptome (Fig. 1 B and Table 2) and applied a step-wise filtering strategy to narrow down potential confounding candidate genes (Fig. 1 C). B6.129-*Prnp^{ZrchI/ZrchI}* pMΦs showed significantly more deviations from the B6 reference than did B6.129-*Prnp^{wt/wt}* (Fig. 1 B and Table 2). By plotting the density of sequence variations in B6.129-*Prnp^{ZrchI/ZrchI}* pMΦ mRNA against their physical location, we observed clustering of variants on chromosome 2 (Chr 2) around *Prnp* at 128–156 Mbp (Fig. 1 B).

Of all genes transcribed in pMΦs, 132 showed nonsynonymous coding variants between B6.129-*Prnp^{wt/wt}* and B6.129-*Prnp^{ZrchI/ZrchI}* (Fig. 1 C and Table S2). Of these, 62 mapped to Chr 2, 4 of which, *Sirpa* (Matozaki et al., 2009; Chao et al., 2012), *Mertk* (Scott et al., 2001), *Tyro3* (Seitz et al., 2007), and *Thbs1* (Gao et al., 1996), had been previously described to impact phagocytosis (Fig. 1 C).

Of these four candidate genes, *Sirpa* (Fig. 1 C) encodes the transmembrane SIRPα, is closely linked to *Prnp* (≈2.2 Mbp), is highly polymorphic in laboratory mice (Sano et al., 1999), and, uniquely among the four candidates, displays polymorphisms with robust modulatory effects on phagocytosis (Takenaka et al., 2007; Legrand et al., 2011; Strowig et al., 2011;

Theocharides et al., 2012; Yamauchi et al., 2013). Binding of CD47 on cognate cells to SIRPα on macrophages transmits a "don't eat me" signal that protects the targets from phagocytosis (Matozaki et al., 2009; Chao et al., 2012). Down-regulation of CD47 cell surface expression on ageing or apoptotic cells enhances their phagocytosis (Barclay and Brown, 2006; Matozaki et al., 2009). Polymorphisms of the Ig-like amino-terminal domain of SIRPα can affect CD47 binding and modulate phagocytosis (Takenaka et al., 2007; Legrand et al., 2011; Strowig et al., 2011; Theocharides et al., 2012). These characteristics led us to prioritize *Sirpa* as the most plausible candidate for modifying the phagocytic phenotype described in B6.129-*Prnp^{ZrchI/ZrchI}* versus B6.129-*Prnp^{wt/wt}* mice.

Sirpa^{129} segregates with *Prnp^−* in seven *Prnp^{−/−}* lines

We then analyzed *Sirpa* alleles in *Prnp^{ZrchI/ZrchI}* mice and in six additional, independently generated mouse lines carrying targeted *Prnp* deletions (Table 1, Fig. 2, and Fig. S1). Restriction fragment length polymorphism (RFLP) analysis and DNA sequencing revealed that the targeted *Prnp* allele co-segregated with the *Sirpa* allele of the 129 strain (*Sirpa^{129}*) in *Prnp^{ZrchI/ZrchI}* mice that had been backcrossed >17 generations to BALB/c (C) or for >12 generations to B6 mice in our colony (Fig. 2). We also observed co-segregation of *Prnp* and *Sirpa* alleles in *Prnp^{ZrchI/ZrchI}* mice backcrossed for 12 generations to B6 and in *Prnp^{Edbg/Edbg}* backcrossed for ≤18 generations to B6 mice from four different laboratories (Figs. S1 and S2 and not depicted). Similar results were observed for alleles at *Mertk*, *Tyro3*, and *Thbs1*, with the exception of an independently generated congenic *Prnp^{−/−}* line called "Ngsk" (Table 1 and Table S3). Congenic B6.129-*Prnp^{Ngsk/Ngsk}* mice have the genotypes *Sirpa^{129/129} Mertk^{129/129} Tyro3^{B6/B6} Thbs1^{B6/B6}*, likely reflecting a recombination event during repeated backcrossing to B6 mice. Thus, *Sirpa* and/or another of the three genes could affect the hyperphagocytosis phenotype reported in *Prnp^{ZrchI/ZrchI}* mice (de Almeida et al., 2005).

Functional analysis excludes *Prnp* and points to *Sirpa* as the gene controlling phagocytosis

We then sought to determine the contribution of polymorphic *Prnp*-flanking genes to the phagocytic phenotype of
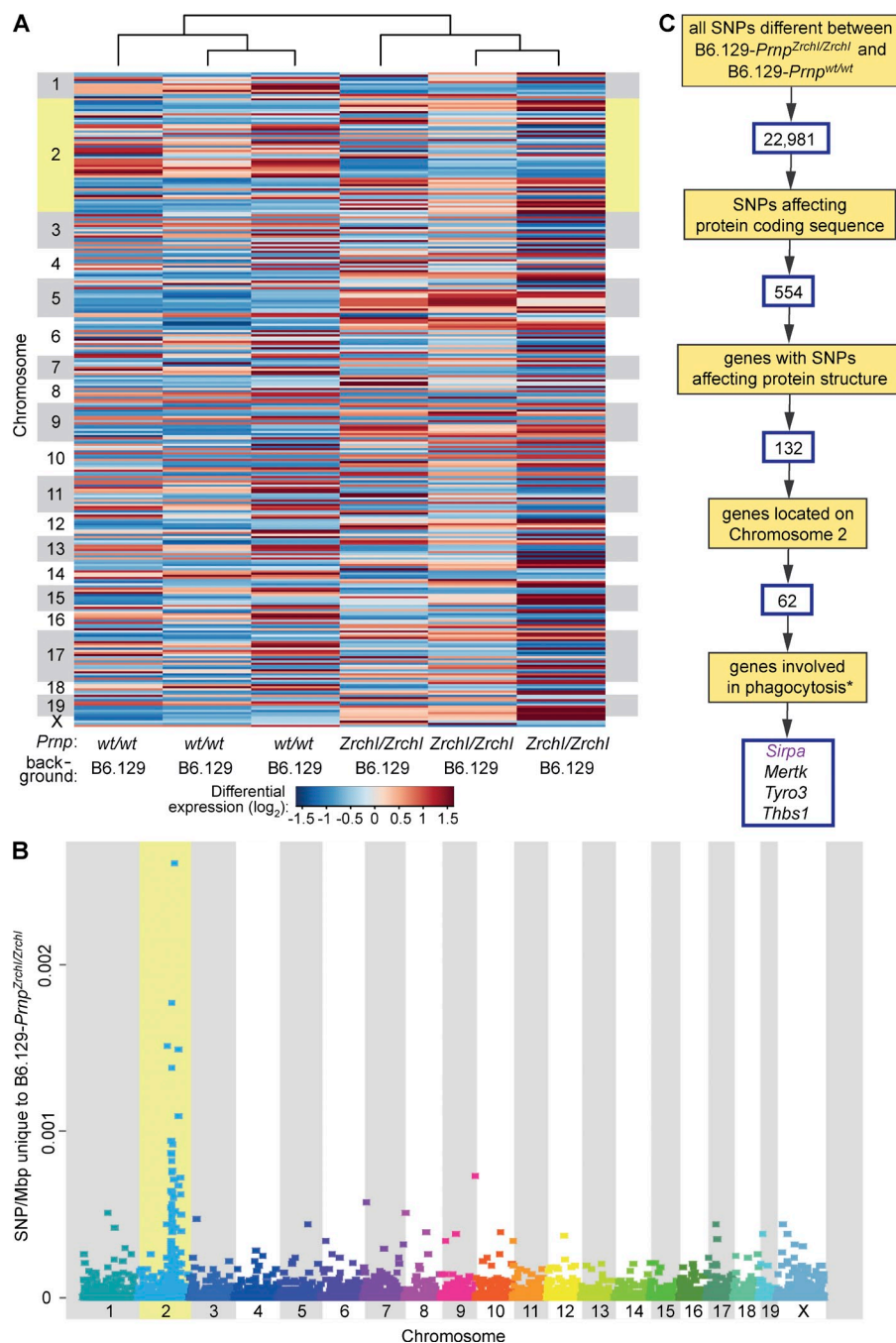
Figure 1.   RNA sequencing identifies macrophage-expressed genes potentially controlling phagocytosis in *Prnp^Zrchl/Zrchl* versus *Prnp^wt/wt* mice. (A) mRNA heat map highlighting 305 differentially expressed genes between B6.129-*Prnp^Zrchl/Zrchl* and B6.129-*Prnp^wt/wt* (pMΦs, three mice per group), ordered by chromosomal location (vertical) and unsupervised hierarchical clustering (horizontal). Chr 2 (in yellow) contains significantly more differentially expressed genes (P = 0.0011, based on Z score > 44 and corrected for chromosome size). Individual genes are listed in Table S1. (B) Physical distribution of SNPs unique to the B6.129-*Prnp^Zrchl/Zrchl* pMΦ transcriptome clustered on Chr 2 (in yellow; two-tailed Student's *t* test, P = 0.019) at 128–156 Mbp. (C) Filtering strategy to prioritize genes controlling phagocytosis in *Prnp^Zrchl/Zrchl* versus *Prnp^wt/wt* mice. Sequential filters were applied to a total of 22,981 SNPs differing between the B6.129-*Prnp^Zrchl/Zrchl* and B6.129-*Prnp^wt/wt* pMΦ transcriptomes. SNPs affecting protein coding sequence included nonsynonymous SNPs and insertions/deletions. The asterisk indicates phenotypic definition based on gene ontology annotations and PubMed searches. *Sirpa*, *Mertk*, *Thbs1*, and *Tyro3* display nonsynonymous SNPs between B6.129-*Prnp^Zrchl/Zrchl* and B6.129-*Prnp^wt/wt* mice, reside on Chr 2, and are involved in phagocytosis. However, only *Sirpa* (purple) is known to display polymorphisms that modulate phagocytosis.

Prnp^−/− mice. The phagocytic activity of primary macrophages was compared between *Prnp^wt/wt* and three different strains of *Prnp^−/−* mice differing at all four, two, or none of the closely linked polymorphic genes. When offered apoptotic thymocytes as targets, B6.129-*Prnp^ZrchI/ZrchI* pMΦs displayed higher rates of phagocytosis than those from heterozygous B6.129-*Prnp^wt/ZrchI* or WT B6.129-*Prnp^wt/wt* congenic littermates (Fig. 3, A and B, left) in agreement with a previous study (de Almeida et al., 2005). We also observed this hyperphagocytic phenotype in BMDMs of B6.129-*Prnp^ZrchI/ZrchI* and B6.129-*Prnp^Ngsk/Ngsk* mice (Fig. 3 B, middle). In contrast, pMΦs from 129-*Prnp^Edbg/Edbg*

mice (Fig. 3 A, right; Manson et al., 1994) displayed similar phagocytic activity as 129-*Prnp^wt/wt* pMΦs (Fig. 3 B, right). 129-*Prnp^Edbg/Edbg* were generated from 129 ES cells and maintained as a co-isogenic 129 line (Fig. 3 A, right). The two strains showed no differences in microsatellite markers linked to *Prnp* (Fig. 3 C). Consequently, ablation of *Prnp* was insufficient to drive hyperphagocytosis, suggesting the influence of additional genetic elements in *Zrchl* and *Ngsk* mice.

To define the 129-derived regions flanking *Prnp*, we performed microsatellite analyses of Chr 2 in B6.129-*Prnp^−/−* mice of the *ZrchI* and *Ngsk* lines. B6.129-*Prnp^ZrchI/ZrchI* mice

Table 2. Summary statistics of RNA sequencing

Mouse	Total reads	Mapped reads	Mean coverage	# SNPs	# Het. SNPs	# Hom. SNPs	# Indels	# Nonsyn. variants	# Nonsyn. variant genes
WT 1	58,838,924	56,801,099 (96.5%)	58.6x	102,465	14,249	88,216	6,860	2,902	362
WT 2	56,971,575	55,447,441 (97.3%)	60.1x	102,756	12,591	90,165	7,451	2,874	361
WT 3	77,632,102	75,325,378 (97.0%)	67.4x	117,354	15,501	101,853	8,356	3,360	415
All WT				84,205	9,535	74,670	5,644	2,277	197
KO 1	71,507,393	69,906,771 (97.8%)	64.6x	117,979	15,146	102,833	8,164	3,517	466
KO 2	70,456,814	68,728,168 (97.5%)	62.7x	114,906	14,943	99,963	8,185	3,391	466
KO 3	75,295,650	73,039,778 (97.0%)	65.4x	117,592	15,539	102,053	8,405	3,515	488
All KO				92,176	9,569	82,607	6,397	2,682	264

WT, B6.129-$Prnp^{wt/wt}$; KO, B6.129-$Prnp^{ZrchI/ZrchI}$; #, number; Het., heterozygous; Hom., homozygous; Indels, insertions/deletions; Nonsyn., nonsynonymous.

harbored 129-derived genomic material in a region of ≥48 Mbp flanking *Prnp* on Chr 2 (including *Sirpa*, *Mertk*, *Tyro3*, and *Thbs1* alleles) despite >12 generations of backcross to B6 (Fig. 3 C and Fig. S2).

Compared with B6.129-$Prnp^{ZrchI/ZrchI}$, B6.129-$Prnp^{Ngsk/Ngsk}$ mice contained a smaller 129-derived interval on Chr 2 (Fig. 3 C). These mice were homozygous for 129 alleles at *Sirpa* and *Mertk* and homozygous for B6 alleles at *Tyro3* and *Thbs1* (Fig. 3 C). Because B6.129-$Prnp^{Ngsk/Ngsk}$ mice retained the hyperphagocytic phenotype, variations in *Tyro3* or *Thbs1* alleles did not explain the differential phagocytic activity of $Prnp^{wt/wt}$ and $Prnp^{-/-}$ mice, excluding these two genes as candidates (Fig. 3 C).

We identified only one nonsynonymous single nucleotide polymorphism (SNP) in $Mertk^{129}$ versus $Mertk^{B6}$ alleles (Chr2: 128776396, Att/Gtt). This SNP, previously reported in CD-1 mice (SNP accession no. rs27446326 from dbSNP Build 137), results in a conservative isoleucine-to-valine substitution within the transmembrane region (I516V) and is predicted by the SIFT algorithm (Ng and Henikoff, 2001; Kumar et al., 2009) to be tolerated and unlikely to impact *Mertk* function. All disease-causing *MERTK* mutations identified so far in patients suffering from retinitis pigmentosa (Gal et al., 2000), Leber congenital amaurosis (Li et al., 2011), or cancer (Greenman et al., 2007) were located in the extracellular or cytoplasmic but not in the transmembrane region. Moreover, one natural
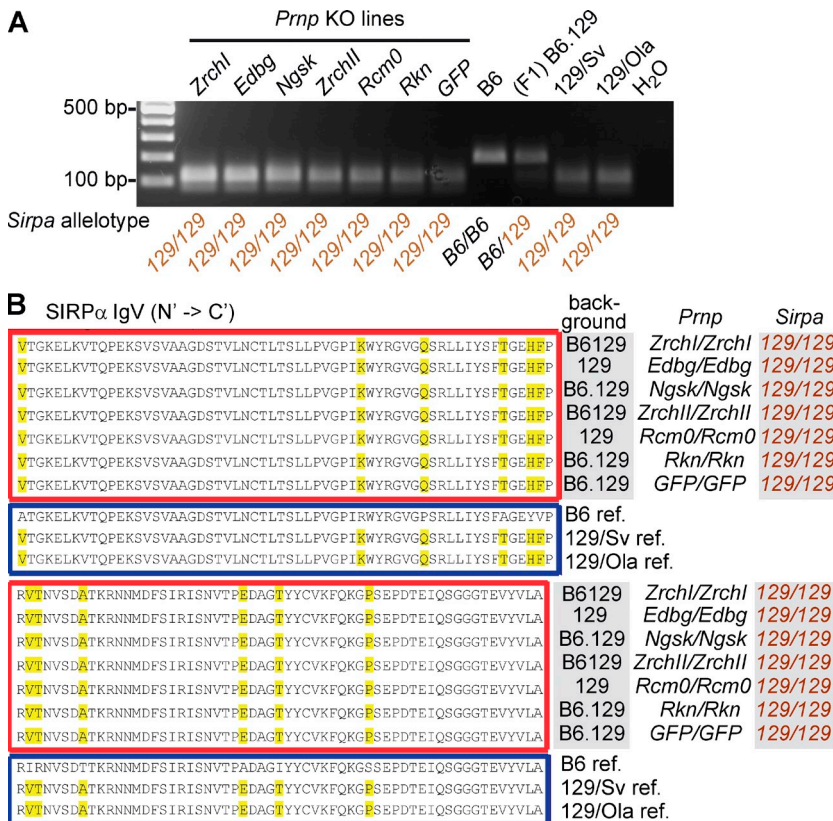
Figure 2. ***Sirpa* allelotype of the *Prnp*$^{-/-}$ lines analyzed in this study.** (A) RFLP analysis of *Sirpa* allelotypes. The *Sirpa*^{129} allele segregates with the *Prnp*$^-$ allele in *Prnp*$^{-/-}$ mouse lines stemming from seven independent targeting events (see Table 1). The 8th through 11th lanes show respective reference strain DNA. (B) The red box indicates protein sequence alignment of mouse SIRPα Ig-like variable domain (IgV) confirming the 129 *Sirpa* allelotype in each one of the seven *Prnp*$^{-/-}$ lines shown in A. The blue box indicates SIRPα protein reference sequences for the B6, 129/Sv, and 129/Ola strains. Polymorphisms are highlighted in yellow. For each group one mouse was analyzed.

SIRPα, not PrP^C, controls phagocytosis | Nuvolone et al.
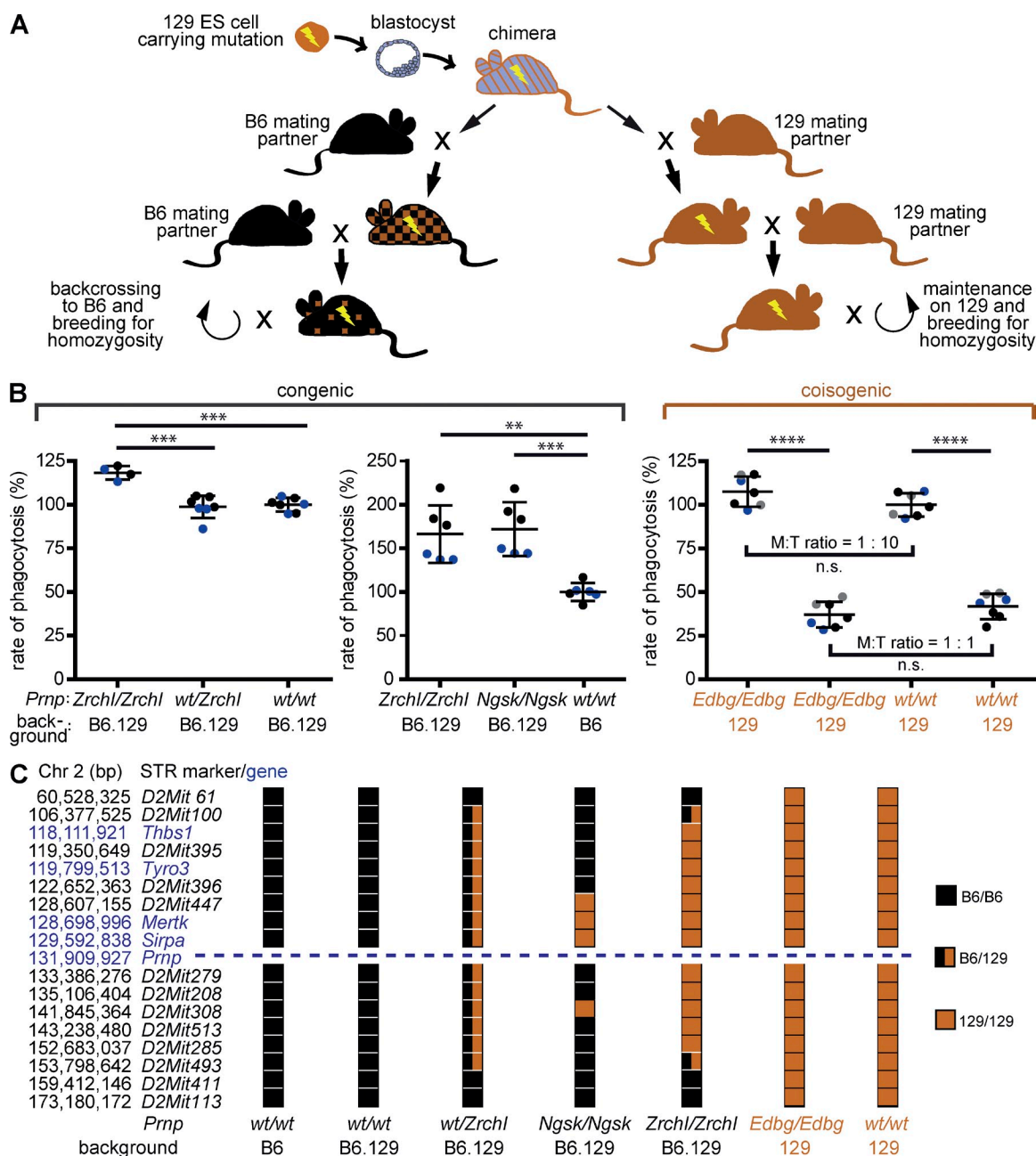
Figure 3. Ablation of *Prnp* is not sufficient to enhance phagocytosis of apoptotic cells. (A) Generation of B6.129 congenic (left) and 129 co-isogenic (right) *Prnp*^{−/−} lines. In B6.129 congenic mice, residual 129 genomic material derived from the ES cell (brown) is inevitably present, particularly in the region flanking the targeted locus. (B, left) pMΦs from congenic B6.129-*Prnp*[Zrchl/Zrchl] mice showed higher phagocytic activity than those from B6.129-*Prnp*[wt/wt] (set as 100%) and B6.129-*Prnp*[wt/Zrchl] littermates. Blue, black, and gray (here and henceforth) indicate data from independent experiments. (middle) B6.129-*Prnp*[Zrchl/Zrchl] and B6.129-*Prnp*[Ngsk/Ngsk] BMDMs showed higher phagocytic activity than B6-*Prnp*[wt/wt] macrophages (set as 100%). (right) The phagocytic activity of 129-*Prnp*[Edbg/Edbg] and 129-*Prnp*[wt/wt] macrophages was similar, even when two different macrophage/thymocyte (M:T) ratios were used (1:10 and 1:1; one-way ANOVA, Bonferroni's multiple comparisons test). Mean 129-*Prnp*[wt/wt] phagocytic rate at 1:10 M:T ratio was set as 100%. n.s., not significant; **, $P < 0.005$; ***, $P < 0.001$; ****, $P < 0.0001$. Error bars indicate SD. (C) STR analysis of Chr 2. Name and physical position of each STR marker (colored boxes) are indicated on the left. B6.129-*Prnp*[Zrchl/Zrchl] and B6.129-*Prnp*[Ngsk/Ngskl] mice contained 129-derived genetic material flanking *Prnp*, whereas the markers flanking *Prnp* in 129-*Prnp*[Edbg/Edbg] and 129-*Prnp*[wt/wt] mice were identical. Data show representative mice of at least three animals analyzed per group.
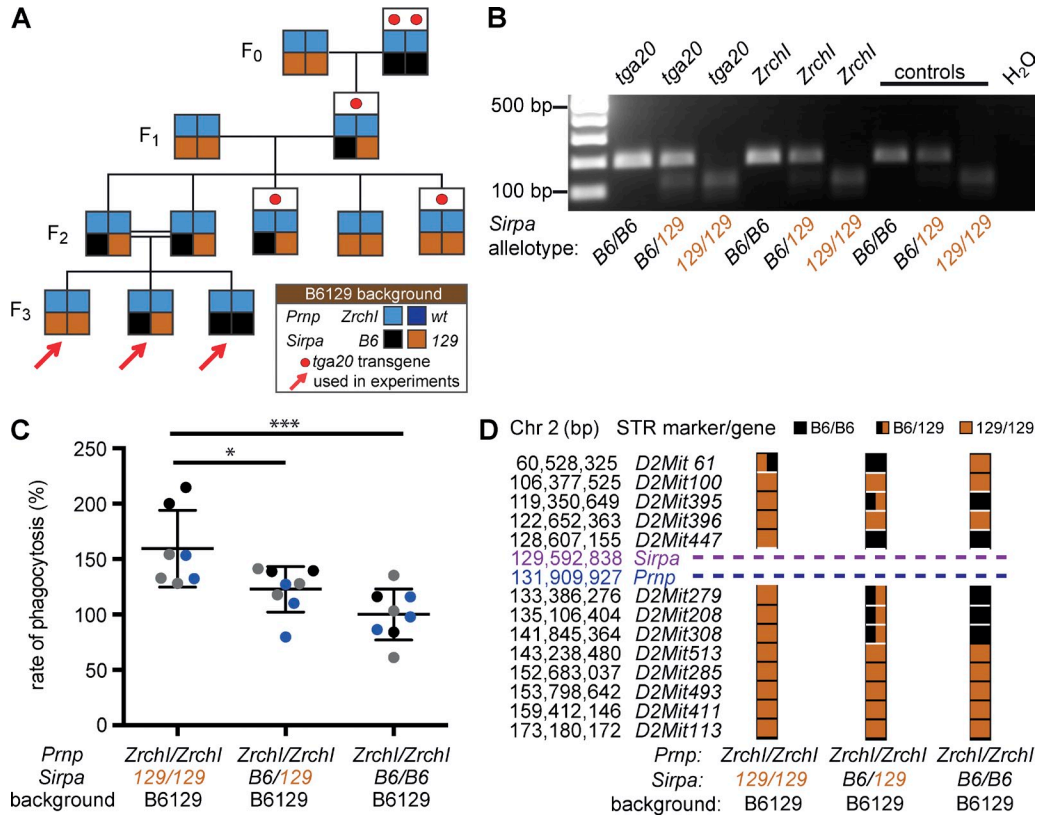
Figure 4. **Sirpa^B6 allele segregates with enhanced inhibition of phagocytosis in the absence of Prnp.** (A) Breeding scheme applied to generate B6129-*Prnp^{ZrchI/ZrchI}* mice containing *Sirpa^{B6}* and *Sirpa^{129}* alleles. B6129-*Prnp^{ZrchI/ZrchI} Sirpa^{B6/B6} tga20^{tg/tg}* mice (F_0) were backcrossed to B6129-*Prnp^{ZrchI/ZrchI} Sirpa^{129/129}* mice for two generations to produce B6129-*Prnp^{ZrchI/ZrchI}* littermates, with all combinations of *Sirpa^{B6}* and *Sirpa^{129}* alleles (F_3) used to assess phagocytic activity as in C. (B) RFLP analysis of *Sirpa* allelotypes (B6 vs. 129). Surprisingly, *tga20* mice (first through third lanes) displayed combinations of *Sirpa^{B6}* and *Sirpa^{129}* alleles. The fourth through sixth lanes show B6129-*Prnp^{ZrchI/ZrchI}* mice labeled in A (red arrows). Controls are reference DNA. All animals entering the study were analyzed. (C) Phagocytic hyperactivity of B6129-*Prnp^{ZrchI/ZrchI}* pMΦs was associated with the *Sirpa^{129/129}* allelotype. Data from three independent experiments (blue, black, and gray) normalized against mean B6129-*Prnp^{ZrchI/ZrchI}Sirpa^{B6/B6}* phagocytic rates. One-way ANOVA, Bonferroni's multiple comparisons test: *, $P < 0.05$; ***, $P < 0.001$. Error bars indicate SD. (D) STR analysis documenting the boundaries of B6 versus 129-derived genome in Chr 2 of B6129-*Prnp^{ZrchI/ZrchI}* with different combinations of *Sirpa* alleles (B6 vs. 129). Name and position of each STR marker (colored box) on Chr 2 are indicated on the left. Data show representative mice of at least three animals analyzed per group.

non–disease-causing variant in the transmembrane region has been reported in humans (I518V; Gal et al., 2000; Li et al., 2011), which corresponds to the I516V variant in our mice, again suggesting that the variant identified in our mice is unlikely to impact *Mertk* function. Collectively, these findings suggested that *Sirpa^{129}* homozygosity conferred differential levels of phagocytosis in otherwise genetically homogeneous mice and that the presence of at least one *Sirpa^{B6}* allele reduced rates of phagocytosis compared with *Sirpa^{129}* homozygotes.

### Sirpa^B6 association with inhibition of phagocytosis
We observed that some of our PrP^C-overexpressing *tga20* transgenic mice on a mixed B6129-*Prnp^{ZrchI/ZrchI}* background (Fischer et al., 1996) were segregating *Sirpa^{B6}* and *Sirpa^{129}* alleles, likely reflecting an unintentional cross with B6-*Prnp^{wt/wt}* breeders in the early days of this colony (unpublished data). We crossed B6129-*Prnp^{ZrchI/ZrchI} Sirpa^{B6/B6} tga20^{tg/tg}* mice to B6129-*Prnp^{ZrchI/ZrchI} Sirpa^{129/129}* mice producing B6129-*Prnp^{ZrchI/ZrchI}* littermates with all three combinations of *Sirpa^{B6}* and *Sirpa^{129}*

alleles (Fig. 4, A and B). pMΦs from B6129–*Prnp^{ZrchI/ZrchI} Sirpa^{129/129}* mice showed higher rates of phagocytosis (Fig. 4, C and D). Hence, compared with *Sirpa^{129/129}*, a single *Sirpa^{B6}* allele reduced phagocytosis rates in the absence of *Prnp*. These results supported the hypothesis that homozygosity for *Sirpa^{129}* rather than *Prnp* deficiency was responsible for the hyperphagocytic phenotype of *Prnp^{ZrchI/ZrchI}* mice.

Inhibition of phagocytosis segregated with Sirpa^B6 in Prnp^{wt/wt} mice
Sirpa alleles and *Prnp* ablation may impact phagocytosis independently of each other. We therefore asked whether different *Sirpa* alleles could modify phagocytosis in *Prnp^{wt/wt}* mice. We genotyped 103 pups from B6.129-*Prnp^{wt/ZrchI} Sirpa^{B6/129}* intercross mice for recombination between *Prnp* and *Sirpa* and observed two events producing a *Prnp^{wt}–Sirpa^{129}* and a *Prnp^{ZrchI}–Sirpa^{B6}* haplotype (Fig. 5 A). Mice carrying the original and the recombinant haplotypes were then bred to generate congenic mice with different *Prnp–Sirpa* haplotypes (Fig. 5, B and C).
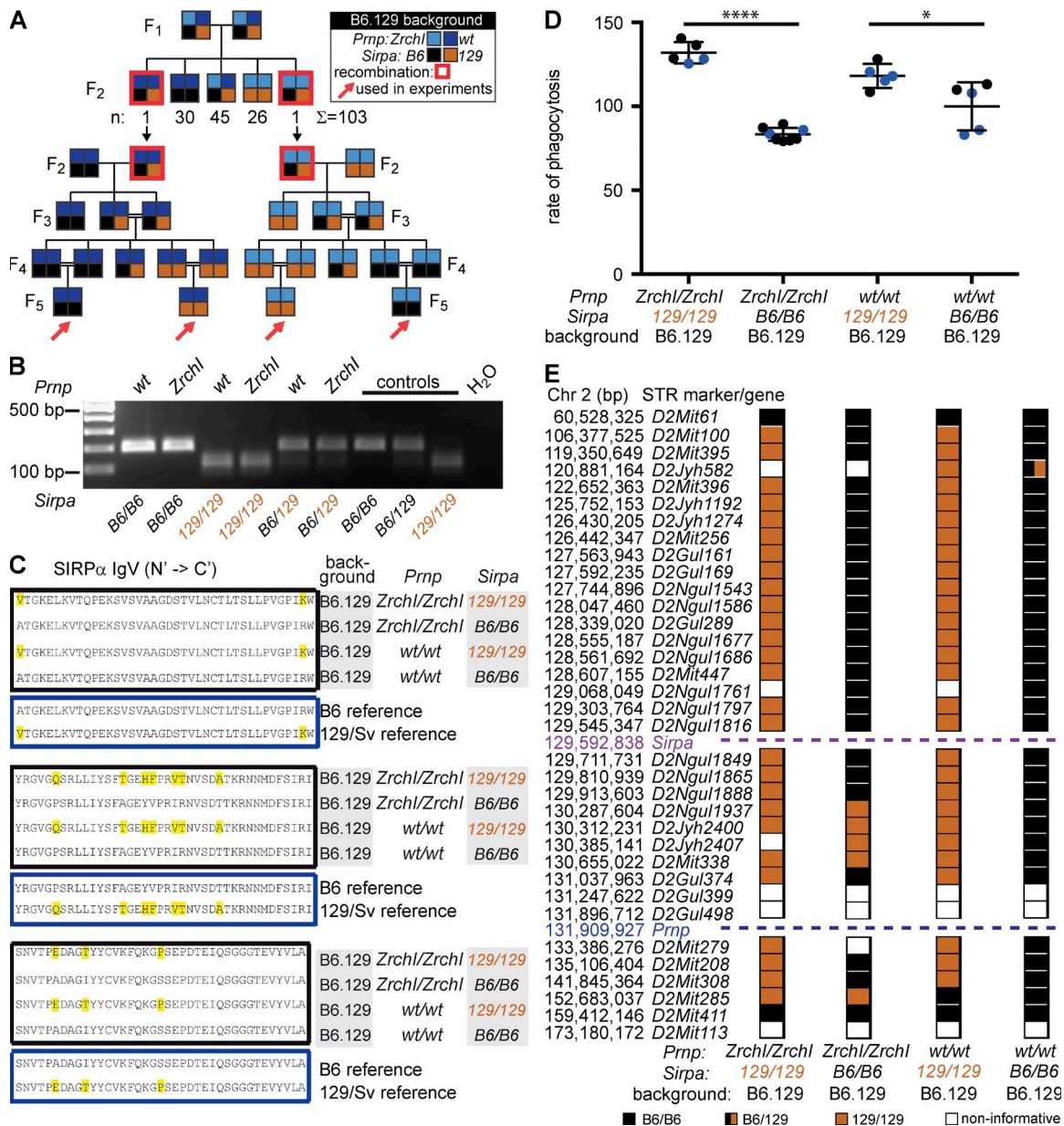
Figure 5. Hyperphagocytosis is associated with the *Sirpa^129/129* allelotype but not with *Prnp* gene dosage. (A) Breeding scheme to generate recombinant congenic B6.129 mice with different combinations of *Prnp* (WT and ZrchI) and *Sirpa* (B6 and 129) alleles. B6.129-*Prnp^wt/ZrchI* mice (F₁) were intercrossed, and F₂ offspring were screened for meiotic recombination between *Prnp* and *Sirpa*. 103 F₂ mice with different combinations of *Prnp* genotypes and *Sirpa* allelotypes were obtained. Two mice (red frames) were found to carry the recombinant haplotype, *Prnp^wt-Sirpa^129* and *Prnp^ZrchI-Sirpa^B6* and were interbred to generate B6.129-*Prnp^ZrchI/ZrchI* and B6.129-*Prnp^wt/wt* mice homozygous for *Sirpa^B6* or *Sirpa^129* alleles. (B) RFLP analysis to discriminate between *Sirpa^129* and *Sirpa^B6*. B6.129-*Prnp^wt/wt* (first, third, and fifth lanes) and B6.129-*Prnp^ZrchI/ZrchI* (second, fourth, and sixth lanes) mice with different combinations of *Sirpa^129* and *Sirpa^B6* alleles. Controls are reference DNA. All animals entering the study were analyzed. (C) Protein sequence variants (yellow) in SIRPα Ig-like variable domain (IgV). Homozygous recombinant congenic B6.129 mice displayed four combinations of *Prnp-Sirpa* haplotypes (black boxes). Blue boxes show SIRPα sequence of reference B6 and 129/Sv strains. For each group one mouse was analyzed. (D) *Sirpa^129/129*, but not *Prnp^-/-*, was associated with hyperphagocytosis in pMΦs from congenic B6.129 mice. Data are from two independent experiments (blue and black); phagocytosis rates were normalized against B6.129 *Prnp^wt/wt Sirpa^B6/B6*. One-way ANOVA, Bonferroni's multiple comparisons post-test: *, P < 0.05; ****, P < 0.0001. Error bars indicate SD. (E) Recombination breakpoints between *Prnp* and *Sirpa* in congenic B6.129 mice. For each STR marker (colored box), name and position on Chr 2 are indicated on the left. Data show representative mice of at least three animals analyzed per group.

The various *Prnp-Sirpa* haplotypes did not affect the frequency of macrophages in peritoneal lavages, nor did *Sirpa* allelotypes affect PrP^C expression (Fig. 6, A–C). Also, we did not observe differences in *Sirpa* mRNA levels between pMΦs from B6.129-*Prnp^ZrchI/ZrchI* and B6.129-*Prnp^wt/wt* mice (375.60 vs. 356.34 fragments per kilobase of transcript per million

mapped reads [FPKM], respectively, P = 0.73) or SIRPα protein levels in mice with different *Prnp-Sirpa* haplotypes (Fig. 6 D). These results excluded any influence of *Prnp* or *Sirpa* alleles on the expression of each other.

In congenic B6.129 mice with different combinations of *Prnp* and *Sirpa* alleles (WT and ZrchI, B6 and 129, respectively), hyperphagocytosis segregated with *Sirpa^{129/129}* irrespectively of the *Prnp* status (Fig. 5, D and E). We compared phagocytosis by BMDMs isolated from congenic C.129-*Prnp^{ZrchI/ZrchI}* mice with different combinations of *Prnp* and *Sirpa* alleles (Fig. 7, A–C). In line with our findings with congenic B6.129 mice, a higher phagocytosis rate correlated with *Sirpa^{129/129}* independently of the *Prnp* alleles (Fig. 7, D and E). Together, these results exclude a role for PrP^C and support *Sirpa* polymorphisms as a major regulator of phagocytosis in mouse strains carrying either WT or deleted *Prnp* alleles.

DISCUSSION

In the 1990s the *Prnp* gene became an extremely popular target among mouse geneticists and rapidly advanced to one of the most frequently inactivated elements of the mouse genome. As a result, we have indeed identified at least seven published mouse lines derived from independent gene-targeting events, all of which were analyzed in the present study. Remarkably, we discovered that all of these lines suffer from the same set of confounders when kept as congenic: a 129-derived genomic region sporting functionally impactful polymorphisms.

The alleged control of phagocytosis of apoptotic cells by *Prnp* was critically questioned when we found that, in contrast to congenic B6.129- or C.129-*Prnp^{ZrchI/ZrchI}* and B6.129-*Prnp^{Ngsk/Ngsk}* mice, co-isogenic 129-*Prnp^{Edbg/Edbg}* mice did not display a hyperphagocytic phenotype. Moreover, microsatellite-assisted breeding of B6129-*Prnp^{ZrchI/ZrchI}* mice revealed the existence of a 129-derived Chr 2 segment which, when homozygous, correlated with a higher rate of phagocytosis independent of *Prnp*. These data suggested that *Prnp* does not impact phagocytosis and that such conclusions in previous studies resulted from unrecognized polymorphic flanking genes (de Almeida et al., 2005). Detailed genomic, transcriptomic, and functional analysis of candidate genes in the introgressed 129-derived region in B6.129–*Prnp^{ZrchI/ZrchI}* mice supported a focus on the well-characterized inhibitor of phagocytosis *Sirpa*, whose polymorphisms alter this phenotype (Takenaka et al., 2007; Legrand et al., 2011; Strowig et al., 2011). Indeed, *Sirpa^{129}*, rather than *Prnp^−*, segregated with increased phagocytosis.

B6.129-*Prnp^{ZrchI/ZrchI}* and B6.129-*Prnp^{wt/wt}* macrophages displayed sequence variations, or differential expression, of several other genes in addition to *Sirpa*. In particular, *Mertk* (Scott et al., 2001), *Tyro3* (Seitz et al., 2007), and *Thbs1* (Gao et al., 1996), which participate in phagocytosis and are linked to *Prnp*, were polymorphic between the two strains. However, the genetic and functional considerations detailed above suggested that they were unlikely candidates.

In our study, we have used mouse genetics to investigate the role of PrP^C and its polymorphic flanking genes in modulating phagocytosis of apoptotic cells. Compared with other experimental approaches, including gene silencing and overexpression of exogenously introduced genes, formal genetics has the advantage of assessing the differential impact of physiological versus absent expression of the gene under scrutiny. Moreover, silencing or overexpressing *Sirpa*, or other modulators of phagocytosis, could alter the delicate balance between pro- and antiphagocytic signals (Hochreiter-Hufford and Ravichandran, 2013) and impact phagocytosis independently of whether this modulator is responsible for the difference between *Prnp^{−/−}* and *Prnp^{+/+}* macrophages.

Enzymatic removal of PrP^C from macrophage surface through phosphoinositol phospholipase C was reported to result in an increased phagocytosis of apoptotic cells, seemingly confirming the role of PrP^C in this process (de Almeida et al., 2005). However, this treatment generically affects all glycosylphosphatidylinositol-anchored proteins, many of which are involved in the control of phagocytosis (Dorahy et al., 1996; Cebecauer et al., 1998; Oliferenko et al., 1999; Kellner-Weibel et al., 2000; Peyron et al., 2000; Chimini, 2001; de Almeida and Linden, 2005). Therefore, it is questionable whether this effect is directly mediated by loss of surface PrP^C.

Our study focused on the presumed role of PrP^C in phagocytosis of apoptotic cells. Phagocytosis of zymosan particles and latex beads were also reported to be influenced by *Prnp* using primary macrophages or immortalized cell lines derived from *Prnp^{−/−}* and *Prnp^{+/+}* mice (de Almeida et al., 2005; Nitta et al., 2009; Uraki et al., 2010). Our results raise the question of whether *Sirpa* polymorphisms may affect the responses to zymosan or phagocytosis of latex beads as well.

The co-segregation of *Sirpa^{129}* with *Prnp^−* in all the *Prnp^{−/−}* lines examined has implications beyond the control of phagocytosis. Because the *Sirpa* sequence of most mouse strains used for backcrossing of *Prnp^{−/−}* mice (B6, BALB/c, and FVB) differs from 129 mice (Sano et al., 1999; Takenaka et al., 2007), *Sirpa* is a potential confounder in most studies of *Prnp^{−/−}* mice. Importantly, the expression pattern of *Sirpa* mirrors that of *Prnp* and includes myeloid cells, neurons, and pancreatic β cells (Linden et al., 2008; Matozaki et al., 2009). Finally, PrP^C-deficient mice share numerous subtle phenotypes with *Sirpa*-ablated mice, including neuroimmunological (Tomizawa et al., 2007; Tsutsui et al., 2008), behavioral (Nico et al., 2005; Ohnishi et al., 2010; Gadotti et al., 2012), and metabolic phenotypes (Kobayashi et al., 2008; Strom et al., 2011). These observations suggest that additional phenotypes attributed to *Prnp* may actually reflect the effects of *Sirpa* polymorphisms.

Based on studies with *Prnp^{−/−}* mice, PrP^C has been recently reported to either induce or inhibit autophagy (Oh et al., 2008, 2012; Korom et al., 2013) and to be indispensable or dispensable to mediate Aβ toxicity (Laurén et al., 2009; Balducci et al., 2010; Calella et al., 2010; Gimbel et al., 2010; Kessels et al., 2010; Cissé et al., 2011; Larson et al., 2012; Um et al., 2012). At least some of these controversies could reflect

SIRPα, not PrP^C, controls phagocytosis | Nuvolone et al.
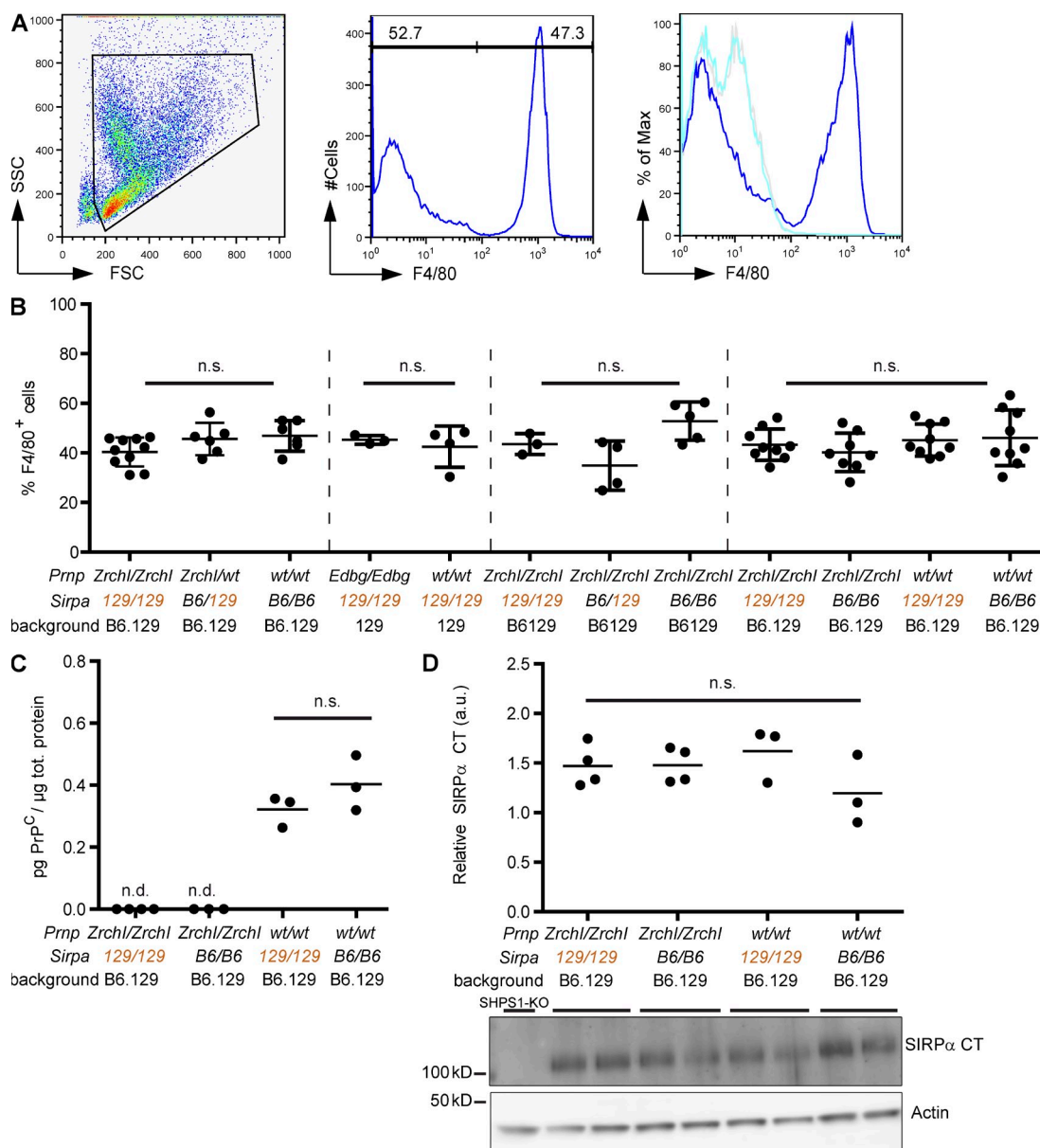
Figure 6.   **Sirpa allelotype does not influence pMΦ abundance or PrP^C and SIRPα expression.** (A) Peritoneal lavages were gated for nucleated cells (left), and the percentage of F4/80+ cells was assessed (middle panel, right peak). (right) Overlay of histograms of F4/80 (dark blue), isotype antibody (light blue), and unstained peritoneal cells (gray) confirming the specificity of the staining. (B) Percentage of F4/80+ macrophages in peritoneal lavage cells of experimental mice. The dotted lines delineate individual experiments in which groups of mice (n = 3–10 for each haplotype) were analyzed. Error bars indicate SD. (C) PrP^C ELISA analysis of pMΦ lysates showed no difference (n.s.) in PrP^C levels between B6.129-*Prnp^{wt/wt}* mice with different *Sirpa* allelotypes. Two-tailed unpaired Student's t test: P = 0.241; n = 3–4 for each haplotype. n.d., not detectable. (D) Unchanged expression of the SIRPα cytoplasmic tail (CT) in cultured pMΦ lysates as quantified to actin levels. SHPS-1 KO macrophage lysates lacking the cytosolic tail of SIRPα were used as negative control. One-way ANOVA: n.s., not significant; P = 0.27; n = 3–4 for each haplotype. Horizontal bars indicate mean.

the effect of polymorphic *Prnp*-flanking genes, and these findings merit critical reconsideration in light of our data.

The risk of flanking-gene problems can be reduced by reversing the phenotype of gene-targeted mice through transgenetic restoration of gene expression (Wolfer et al., 2002). With *Prnp*, this was often done by using PrP^C-overexpressing *tga20* mice, which were generated from *Prnp^{ZrchI/ZrchI}* mice and subsequently distributed to many laboratories. However, we

found that the *tga20* colony was contaminated with multiple combinations of *Sirpa* alleles early after its establishment. Hence the rescue of *Prnp* deficiency through a *tga20* allele does not necessarily prove that the observed changes in phenotype are PrP^C dependent.

It has been long suspected that genes flanking targeted loci may confound the interpretation of KO experiments (Smithies and Maeda, 1995; Gerlai, 1996). Recommendations
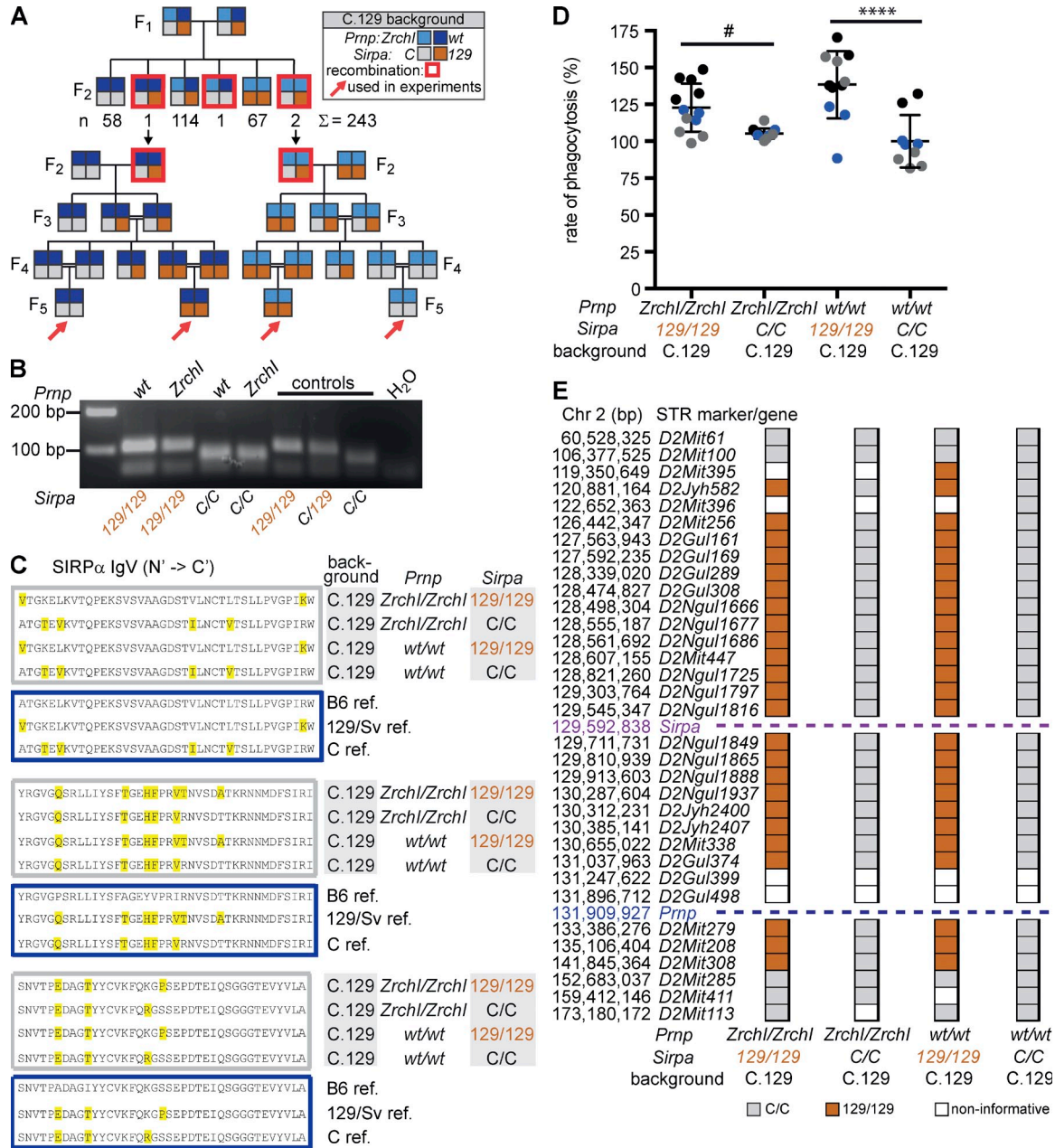
Figure 7. Phagocytic activity level is associated with *Sirpa^129/129* allelotype but not with *Prnp* gene dosage also in C.129 congenic mice. (A) Breeding scheme to generate recombinant congenic C.129 mice with different combinations of *Prnp* (WT and Zrchl) and *Sirpa* (C and 129) alleles. C.129-*Prnp^wt/Zrchl* mice (F_1) were intercrossed, and the occurrence of meiotic recombination between *Prnp* and *Sirpa* was assessed in the F_2 offspring. 243 F_2 mice with different combinations of *Prnp* genotypes and *Sirpa* allelotypes were obtained. Four mice (red frames) were found to carry a recombinant haplotype, and selected ones were bred to generate C.129-*Prnp^Zrchl/Zrchl* and C.129-*Prnp^wt/wt* mice homozygous for *Sirpa^C* or *Sirpa^129* alleles. (B) RFLP analysis used to discriminate *Sirpa^129* from *Sirpa^C* alleles. C.129-*Prnp^wt/wt* (first, third, and fifth lanes) and C.129-*Prnp^Zrchl/Zrchl* (second, fourth, and sixth lanes) mice with different combinations of *Sirpa^129* and *Sirpa^C* alleles. Controls are reference DNA. All animals entering the study were analyzed. (C) Protein sequence alignment of mouse SIRPα Ig-like variable domain (IgV) illustrates recombinant congenic C.129 mice with different combinations of *Prnp* and *Sirpa^129* versus *Sirpa^C* (gray border). Blue boxes are SIRPα protein reference sequences for the B6, 129/Sv, and C strains (yellow: polymorphisms). For each group one mouse was analyzed. (D) *Sirpa^129/129* allelotype, but not the absence of *Prnp*, was associated with hyperphagocytosis of BMDMs in congenic C.129 mice. Data are from three independent experiments (blue, black, and gray). Mean phagocytosis rates of C.129 *Prnp^Zrchl/Zrchl* *Sirpa^B6/B6* were set as 100%. One-way ANOVA, Bonferroni's multiple comparison post-test: #, P = 0.075; ****, P < 0.0001. Error bars indicate SD. (E) STR analysis documents the result of trans-allelic meiotic recombination between *Prnp* and *Sirpa*. Blue dashed line indicates the location of *Prnp* and *Sirpa*. For each STR marker (colored box), name and position on Chr 2 are indicated on the left. Data show representative mice of at least three animals analyzed per group.

for breeding schemes and genetic quality control to avoid this problem were formulated (Wolfer et al., 2002; Ridgway et al., 2007; Crusio et al., 2009) but rarely implemented (Holmdahl and Malissen, 2012). Consequently, reports of flanking gene effects are anecdotal and rely on the demonstration that a KO mouse phenotype is lost upon crossing to other strains backgrounds and reduction in length of the 129-derived region flanking the targeted locus (Kanagawa et al., 2000; de Ledesma et al., 2006; Eisener-Dorman et al., 2010). Our findings provide an alternative mechanism underlying prior specific claims in the prion field and strengthen the requirement for rigorous genetic, genomic, and functional analyses to support the assignment of specific phenotypes to targeted mutations in mice.

MATERIALS AND METHODS

Mice. The following mice were analyzed: $Prnp^{ZrchI/ZrchI}$ mice (Büeler et al., 1992) on a mixed B6129 background or backcrossed to B6 for >12 generations or to C for >17 generations and congenic WT B6 and C mice purchased from Harlan or Charles River or bred in house; $Prnp^{Ngsk/Ngsk}$ mice (Sakaguchi et al., 1995) extensively backcrossed to B6; $Prnp^{Edbg/Edbg}$ mice on a pure 129/Ola background (Manson et al., 1994) and co-isogenic WT 129/Ola mice; $Prnp^{ZrchII/ZrchII}$ mice (Rossi et al., 2001) on a mixed B6129 background; $Prnp^{GFP/GFP}$ mice (Heikenwalder et al., 2008) backcrossed to B6 for 10 generations; $tga20$ mice (Fischer et al., 1996) on a mixed B6129 $Prnp^{ZrchI/ZrchI}$ background; and SHPS-1 (Inagaki et al., 2000) backcrossed to B6 for >5 generations. Genotype of mice was verified as indicated in the original description of each line (Table 1). To introduce $Sirpa^{B6}$ into B6129-$Prnp^{ZrchI/ZrchI}$ mice, B6129-$Prnp^{ZrchI/ZrchI}$ $Sirpa^{B6/B6}$ $tga20^{tg/tg}$ mice were crossed with B6129-$Prnp^{ZrchI/ZrchI}$ $Sirpa^{129/129}$ mice (Fig. 4 A). To generate congenic B6.129-$Prnp^{ZrchI/ZrchI}$ and $Prnp^{wt/wt}$ mice with all possible combinations of $Sirpa^{B6}$ and $Sirpa^{129}$ alleles, B6.129-$Prnp^{wt/ZrchI}$ $Sirpa^{B6/129}$ mice were intercrossed, and recombination events between $Prnp$ and $Sirpa$ loci were identified by $Prnp$ genotyping and RFLP analysis of $Sirpa$ exon 2 in the offspring (Fig. 5, A and B). Mice with a recombinant haplotype (referred to as obligate carriers) were further crossed. The same approach was followed to generate congenic C.129-$Prnp^{ZrchI/ZrchI}$ and $Prnp^{wt/wt}$ mice with all possible combinations of $Sirpa^C$ and $Sirpa^{129}$ alleles (Fig. 7, A and B). All animal experiments were performed in compliance with the Swiss Animal Protection Law, under the approval of the Veterinary office of the Canton Zurich.

Allele discrimination analysis. To distinguish strain-specific alleles, PCR-RFLP analysis (*Sirpa*, *Tyro3*, and *Thbs1*) or sequencing (*Mertk*) were performed using primers and restriction enzymes as detailed in Table S4.

Phagocytosis assay with pMΦs. On day 0, peritoneal cells were collected from age- and gender-matched adult mice according to standard methods (Fortier and Falk, 2001), resuspended to 2.2×10^6 in 5 ml DMEM (Gibco) with 10% FBS (Gibco), 1% GlutaMAX (Gibco), and antibiotics, plated in one-well slide chambers (Falcon; BD), and incubated at 37°C. After 2 h, nonadhering cells were removed and remaining cells (referred to as cultured pMΦs) were kept overnight in culture. On day 1, thymocytes were harvested from 3–8-wk-old mice of the same background as the genotypes under investigation, incubated for 3 h at 37°C in the presence of 1 µM dexamethasone to induce apoptosis, washed, and added to the cultured pMΦs at different ratios for 1 h. For each experimental group, technical replicates (at least duplicates) were performed. Cells were washed, fixed with formalin, and stained with May-Grünwald-Giemsa. Slides were randomized and scanned with NanoZoomer (Hamamatsu Photonics), random fields (50 fields/slide) were generated, and phagocytosis rate was assessed using in-house–developed software. The same operator blinded to experimental groups validated all software-analyzed slides. For each technical replicate, >800 cells were evaluated (indicated as a dot in the graphs). Phagocytosis rate was defined as the percentage of macrophages having at least one apoptotic body.

Phagocytosis assay with BMDMs. On day 0, femurs were collected from age- and gender-matched adult mice and flushed with RPMI1640 medium (Gibco) containing 10% FBS (Gibco), 1% GlutaMAX (Gibco), and antibiotics. BM cells were plated into 6-well plates at 2×10^6/well in 3 ml of culture medium containing 10 ng/ml of macrophage colony stimulation factor (Invitrogen) and cultured overnight at 37°C. On day 1, cells were transferred to new 6-well plates to remove loosely adherent stroma-like cells. On day 6, cells were harvested, adjusted to 5×10^5 cells in 500 µl, and plated into 24-well plates. Apoptotic thymocytes (see above) were suspended at 10^6/ml in PBS and labeled with 20 ng/ml of the pH-sensitive dye pHrodo red, SE (Invitrogen) for 30 min at room temperature and washed, and 500 µl of cell suspension was added to BMDM culture for 1 h at 37°C. After washing, BMDMs were harvested with Accutase (Invitrogen) and gentle scraping and stained with FITC-labeled anti-CD11b or isotype control antibody (BD), and rate of phagocytosis was analyzed by flow cytometry as the percentage of pHrodo positivity among CD11b^{+} cells. At least 10,000 events were acquired in the living gate.

Genome-wide and Chr 2 short tandem repeat (STR) analysis. Genome-wide STR analysis was performed as previously described (Bremer et al., 2010). In brief, purified genomic DNA (gDNA) was amplified using multiplex PCR with fluorescently labeled primers (FAM, NED, and VIC; Applied Biosystems), diluted, denatured, and subjected to capillary electrophoresis on a 3130*xl* Genetic Analyzer (Applied Biosystems). Various mouse strains were used for calibration. Peak detection, binning, and allele calling were performed using the GeneMapper software (Applied Biosystems) in combination with in-house–developed software.

High-resolution STR genotyping on Chr 2. Novel microsatellite markers were generated as previously described (Ivakine et al., 2006; primer sequences in Table S4). DNA was amplified for 35 cycles: 30 s at 94°C, 30 s at 55°C, and 1 min at 72°C using Multiplex Master Mix (QIAGEN). The PCR product was diluted 1/20, and 1 µl mixed with a 10-µl mixture containing formamide and a 500LIZ size standard. Samples were resolved on the 3730*xl* DNA Analyzer (Applied Biosystems). Alleles were sized, in comparison with standards, by viewing electropherograms in GeneMapper.

Library preparation for RNA sequencing. Total RNA was isolated from cultured pMΦs using the RNeasy mini kit (QIAGEN), snap frozen, and kept at −80°C until further analysis. RNA quality was determined with Qubit (1.0) Fluorometer (Life Technologies) and Bioanalyzer 2100 (Agilent Technologies). Only samples with a 260 nm/280 nm ratio between 1.8 and 2.1 and a 28S/18S ratio between 1.5 and 2 were further processed. The TruSeq RNA Sample Prep kit v2 (Illumina) was used in the succeeding steps. In brief, total RNA samples (1 µg) were poly A enriched and reverse transcribed into double-stranded cDNA. TruSeq adapters were ligated to double-stranded cDNA. Fragments containing TruSeq adapters on both ends were selectively enriched with PCR. Quality and quantity of enriched libraries were validated using Qubit (1.0) Fluorometer and Caliper GX LabChip GX (Caliper Life Sciences). The product is a smear with a mean fragment size of ∼260 bp. Libraries were normalized to 10 nM in Tris-Cl 10 mM, pH 8.5, with 0.1% (vol/vol) Tween 20.

Cluster generation and RNA sequencing. TruSeq PE Cluster kit v3-cBot-HS (Illumina) was used for cluster generation using 2 pM of pooled normalized libraries on the cBOT. Sequencing was performed on Illumina HiSeq 2000 paired-end at 2×101 bp using the TruSeq SBS kit v3-HS (Illumina). Sequences have been deposited in NCBI Sequence Read Archive under SRA identifier no. SRP029761.

RNA sequencing data analysis. Reads were quality-checked with FastQC. Low-quality ends were clipped (3 bases from the start, 10 bases from the end). Trimmed reads were aligned to the reference genome and transcriptome (FASTA and GIFF files, respectively, downloaded from the UCSC mm10 database) with TopHat version 2.0.6. TopHat was run with the following options: mate inner distance set to 30, the corresponding SD to 100, and

maximum 10 multi-hits were allowed in the alignment. Reads that did not align at the first attempt were split into 25-base-long sections on which a second attempt of alignment was performed. In B6.129-*Prnp*$^{Zrch1/Zrch1}$ pMΦs, all reads mapping to *Prnp* between BstEII and EcoRI restriction sites in exon 3 and in the 3′ UTR, respectively, possibly representing a fused mRNA containing *neo* and residual *Prnp*, reported in the brain of these mice (Büeler et al., 1992), were excluded from the analysis. Polymorphisms were detected using GATK version 2.1.8 using the following options: baq Gap open penalty (whole-genome analysis) set to 30; minimum consensus coverage to genotype indels set to 8 (default: 5); minimum base quality score and minimum variants phred score set to 15. Variants were annotated using snpEFF version 3.0, and distribution of the reads across genomic isoform expression was quantified using RSEM (Li and Dewey, 2011). Cufflinks version 2.0.2 and differentially expressed genes listed with its utility Cuffdiff using default options were used.

All remaining data and statistical analyses, formatting, and picture generating were produced via in-house R-scripts (R version 2.15.2). The SIFT algorithm with default settings was used to predict the impact of a nonsynonymous SNP in *Mertk* (Kumar et al., 2009).

***Sirpa* open reading frame sequencing.** Cultured pMΦ cDNA and gDNA were used to PCR amplify and sequence coding and untranslated regions of mouse *Sirpa* as previously described (Takenaka et al., 2007). Primers (Microsynth) are listed in Table S4. For *Prnp*$^{Rkn/Rkn}$ mice, sequencing was performed on gDNA obtained from Institute of Physical and Chemical Research, Japan, and from cDNA isolated from *Prnp*$^{Rkn/Rkn}$–derived hippocampal like cells (HpL3-4; Kuwahara et al., 1999). For *Prnp*$^{Rem0/Rem0}$ mice, only gDNA from one single mouse was available, and sequencing was performed only on the highly polymorphic exon 2 of *Sirpa*.

Western blotting. Western blotting on pMΦ cell lysates was performed according to standard methods using polyclonal anti–*Sirpa* cytoplasmic tail (CT) antibody (IMGENEX).

PrP^C–ELISA. PrP^C was quantified in cultured pMΦ lysates by sandwich ELISA as described previously using POM1 and POM2 antibodies (Polymenidou et al., 2008).

Flow cytometry analysis. Freshly isolated peritoneal cells were incubated with FITC-labeled anti–F4/80 or isotype control antibody (BD). Thymocyte apoptosis was assessed using the FITC Annexin V Apoptosis Detection kit II (BD). Flow cytometry was performed using a FACSCalibur or a FACSCanto (BD), and data were acquired with CellQuest Pro or FACSDiva software, respectively, and analyzed with FlowJo software (Tree Star).

Statistical analysis. Comparisons of phagocytic activity of macrophages of different genotypes were performed using one-way ANOVA and Bonferroni's multiple comparison post-test (α level 0.05) or two-tailed unpaired Student's *t* test using Prism software (GraphPad Software). The statistical test, p-values, and the *n* for each statistical analysis are indicated in each of the corresponding figure legends.

Online supplemental material. Figs. S1 and S2 illustrate the genomic characterization of experimental mice. Tables S1 and S2, included as separate PDF files, list relevant genes identified by RNA sequencing. Table S3 lists allelotypes of experimental mice. Table S4 lists primer sequences and restriction enzymes used for genetic analysis. Online supplemental material is available at http://www.jem.org/cgi/content/full/jem.20131274/DC1.

REFERENCES

Aguzzi, A., and A.M. Calella. 2009. Prions: protein aggregation and infectious diseases. *Physiol. Rev.* 89:1105–1152. http://dx.doi.org/10.1152/physrev.00006.2009

Balducci, C., M. Beeg, M. Stravalaci, A. Bastone, A. Sclip, E. Biasini, L. Tapella, L. Colombo, C. Manzoni, T. Borsello, et al. 2010. Synthetic amyloid-beta oligomers impair long-term memory independently of cellular prion protein. *Proc. Natl. Acad. Sci. USA.* 107:2295–2300. http://dx.doi.org/10.1073/pnas.0911829107

Barclay, A.N., and M.H. Brown. 2006. The SIRP family of receptors and immune regulation. *Nat. Rev. Immunol.* 6:457–464. http://dx.doi.org/10.1038/nri1859

Bremer, J., F. Baumann, C. Tiberi, C. Wessig, H. Fischer, P. Schwarz, A.D. Steele, K.V. Toyka, K.A. Nave, J. Weis, and A. Aguzzi. 2010. Axonal prion protein is required for peripheral myelin maintenance. *Nat. Neurosci.* 13:310–318. http://dx.doi.org/10.1038/nn.2483

Büeler, H.R., M. Fischer, Y. Lang, H. Bluethmann, H.P. Lipp, S.J. DeArmond, S.B. Prusiner, M. Aguet, and C. Weissmann. 1992. Normal development and behaviour of mice lacking the neuronal cell-surface PrP protein. *Nature.* 356:577–582. http://dx.doi.org/10.1038/356577a0

Calella, A.M., M. Farinelli, M. Nuvolone, O. Mirante, R. Moos, J. Falsig, I.M. Mansuy, and A. Aguzzi. 2010. Prion protein and Abeta–related synaptic toxicity impairment. *EMBO Mol Med.* 2:306–314. http://dx.doi.org/10.1002/emmm.201000082

Cebecauer, M., J. Cerný, and V. Horejsí. 1998. Incorporation of leucocyte GPI-anchored proteins and protein tyrosine kinases into lipid-rich membrane domains of COS-7 cells. *Biochem. Biophys. Res. Commun.* 243:706–710. http://dx.doi.org/10.1006/bbrc.1998.8149

Chao, M.P., I.L. Weissman, and R. Majeti. 2012. The CD47-SIRPα pathway in cancer immune evasion and potential therapeutic implications. *Curr. Opin. Immunol.* 24:225–232. http://dx.doi.org/10.1016/j.coi.2012.01.010

Chimini, G. 2001. Engulfing by lipids: a matter of taste? *Cell Death Differ.* 8:545–548. http://dx.doi.org/10.1038/sj.cdd.4400833

Cissé, M., P.E. Sanchez, D.H. Kim, K. Ho, G.Q. Yu, and L. Mucke. 2011. Ablation of cellular prion protein does not ameliorate abnormal neural network activity or cognitive dysfunction in the J20 line of human amyloid precursor protein transgenic mice. *J. Neurosci.* 31:10427–10431. http://dx.doi.org/10.1523/JNEUROSCI.1459-11.2011

Collinge, J., M.A. Whittington, K.C. Sidle, C.J. Smith, M.S. Palmer, A.R. Clarke, and J.G. Jefferys. 1994. Prion protein is necessary for normal synaptic function. *Nature.* 370:295–297. http://dx.doi.org/10.1038/370295a0

Crusio, W.E., D. Goldowitz, A. Holmes, and D. Wolfer. 2009. Standards for the publication of mouse mutant studies. *Genes Brain Behav.* 8:1–4. http://dx.doi.org/10.1111/j.1601-183X.2008.00438.x

de Almeida, C.J., and R. Linden. 2005. Phagocytosis of apoptotic cells: a matter of balance. *Cell. Mol. Life Sci.* 62:1532–1546. http://dx.doi.org/10.1007/s00018-005-4511-y

de Almeida, C.J., L.B. Chiarini, J.P. da Silva, P.M. E Silva, M.A. Martins, and R. Linden. 2005. The cellular prion protein modulates phagocytosis and inflammatory response. *J. Leukoc. Biol.* 77:238–246. http://dx.doi.org/10.1189/jlb.1103531

de Ledesma, A.M., A.N. Desai, V.J. Bolivar, D.J. Symula, and L. Flaherty. 2006. Two new behavioral QTLs, Emo4 and Reb1, map to mouse Chromosome 1: Congenic strains and candidate gene identification studies. *Mamm. Genome.* 17:111–118. http://dx.doi.org/10.1007/s00335-005-0107-y

Dorahy, D.J., L.F. Lincz, C.J. Meldrum, and G.F. Burns. 1996. Biochemical isolation of a membrane microdomain from resting platelets highly enriched in the plasma membrane glycoprotein CD36. *Biochem. J.* 319:67–72.

Eisener-Dorman, A.F., D.A. Lawrence, and V.J. Bolivar. 2010. Behavioral and genetic investigations of low exploratory behavior in Il18r1(-/-) mice: we can't always blame it on the targeted gene. *Brain Behav. Immun.* 24:1116–1125. http://dx.doi.org/10.1016/j.bbi.2010.05.002

Fischer, M., T. Rülicke, A. Raeber, A. Sailer, M. Moser, B. Oesch, S. Brandner, A. Aguzzi, and C. Weissmann. 1996. Prion protein (PrP) with amino-proximal deletions restoring susceptibility of PrP knockout mice to scrapie. *EMBO J.* 15:1255–1264.

Fortier, A.H., and L.A. Falk. 2001. Isolation of murine macrophages. *Curr. Protoc. Immunol.* Chapter 14:Unit 14.1.

Gadotti, V.M., S.P. Bonfield, and G.W. Zamponi. 2012. Depressive-like behaviour of mice lacking cellular prion protein. *Behav. Brain Res.* 227:319–323. http://dx.doi.org/10.1016/j.bbr.2011.03.012

Gal, A., Y. Li, D.A. Thompson, J. Weir, U. Orth, S.G. Jacobson, E. Apfelstedt-Sylla, and D. Vollrath. 2000. Mutations in MERTK, the human orthologue of the RCS rat retinal dystrophy gene, cause retinitis pigmentosa. *Nat. Genet.* 26:270–271. http://dx.doi.org/10.1038/81555

Gao, A.G., F.P. Lindberg, M.B. Finn, S.D. Blystone, E.J. Brown, and W.A. Frazier. 1996. Integrin-associated protein is a receptor for the C-terminal domain of thrombospondin. *J. Biol. Chem.* 271:21–24. http://dx.doi.org/10.1074/jbc.271.1.21

Gerlai, R. 1996. Gene-targeting studies of mammalian behavior: is it the mutation or the background genotype? *Trends Neurosci.* 19:177–181. http://dx.doi.org/10.1016/S0166-2236(96)20020-7

Gimbel, D.A., H.B. Nygaard, E.E. Coffey, E.C. Gunther, J. Laurén, Z.A. Gimbel, and S.M. Strittmatter. 2010. Memory impairment in transgenic Alzheimer mice requires cellular prion protein. *J. Neurosci.* 30:6367–6374. http://dx.doi.org/10.1523/JNEUROSCI.0395-10.2010

Greenman, C., P. Stephens, R. Smith, G.L. Dalgliesh, C. Hunter, G. Bignell, H. Davies, J. Teague, A. Butler, C. Stevens, et al. 2007. Patterns of somatic mutation in human cancer genomes. *Nature.* 446:153–158. http://dx.doi.org/10.1038/nature05610

Heikenwalder, M., M.O. Kurrer, I. Margalith, J. Kranich, N. Zeller, J. Haybaeck, M. Polymenidou, M. Matter, J. Bremer, W.S. Jackson, et al. 2008. Lymphotoxin-dependent prion replication in inflammatory stromal cells of granulomas. *Immunity.* 29:998–1008. http://dx.doi.org/10.1016/j.immuni.2008.10.014

Hochreiter-Hufford, A., and K.S. Ravichandran. 2013. Clearing the dead: apoptotic cell sensing, recognition, engulfment, and digestion. *Cold Spring Harb. Perspect. Biol.* 5:a008748. http://dx.doi.org/10.1101/cshperspect.a008748

Holmdahl, R., and B. Malissen. 2012. The need for littermate controls. *Eur. J. Immunol.* 42:45–47. http://dx.doi.org/10.1002/eji.201142048

Inagaki, K., T. Yamao, T. Noguchi, T. Matozaki, K. Fukunaga, T. Takada, T. Hosooka, S. Akira, and M. Kasuga. 2000. SHPS-1 regulates integrin-mediated cytoskeletal reorganization and cell motility. *EMBO J.* 19:6721–6731. http://dx.doi.org/10.1093/emboj/19.24.6721

Ivakine, E.A., O.M. Gulban, S.M. Mortin-Toth, E. Wankiewicz, C. Scott, D. Spurrell, A. Canty, and J.S. Danska. 2006. Molecular genetic analysis of the Idd4 locus implicates the IFN response in type 1 diabetes susceptibility in nonobese diabetic mice. *J. Immunol.* 176:2976–2990.

Kanagawa, O., G. Xu, A. Tevaarwerk, and B.A. Vaupel. 2000. Protection of nonobese diabetic mice from diabetes by gene(s) closely linked to IFN-gamma receptor loci. *J. Immunol.* 164:3919–3923.

Kellner-Weibel, G., M. de La Llera-Moya, M.A. Connelly, G. Stoudt, A.E. Christian, M.P. Haynes, D.L. Williams, and G.H. Rothblat. 2000. Expression of scavenger receptor BI in COS-7 cells alters cholesterol content and distribution. *Biochemistry.* 39:221–229. http://dx.doi.org/10.1021/bi991666c

Kessels, H.W., L.N. Nguyen, S. Nabavi, and R. Malinow. 2010. The prion protein as a receptor for amyloid-beta. *Nature.* 466:E3–E4. http://dx.doi.org/10.1038/nature09217

Kobayashi, M., H. Ohnishi, H. Okazawa, Y. Murata, Y. Hayashi, H. Kobayashi, T. Kitamura, and T. Matozaki. 2008. Expression of Src homology 2 domain-containing protein tyrosine phosphatase substrate-1 in pancreatic beta-Cells and its role in promotion of insulin secretion and protection against diabetes. *Endocrinology.* 149:5662–5669. http://dx.doi.org/10.1210/en.2008-0236

Korom, M., K.M. Wylie, H. Wang, K.L. Davis, M.S. Sangabathula, G.S. Delassus, and L.A. Morrison. 2013. A proautophagic antiviral role for the cellular prion protein identified by infection with a herpes simplex virus 1 ICP34.5 mutant. *J. Virol.* 87:5882–5894. http://dx.doi.org/10.1128/JVI.02559-12

Kumar, P., S. Henikoff, and P.C. Ng. 2009. Predicting the effects of coding non-synonymous variants on protein function using the SIFT algorithm. *Nat. Protoc.* 4:1073–1081. http://dx.doi.org/10.1038/nprot.2009.86

Kuwahara, C., A.M. Takeuchi, T. Nishimura, K. Haraguchi, A. Kubosaki, Y. Matsumoto, K. Saeki, Y. Matsumoto, T. Yokoyama, S. Itohara, and T. Onodera. 1999. Prions prevent neuronal cell-line death. *Nature.* 400:225–226. http://dx.doi.org/10.1038/22241

Larson, M., M.A. Sherman, F. Amar, M. Nuvolone, J.A. Schneider, D.A. Bennett, A. Aguzzi, and S.E. Lesné. 2012. The complex PrP(c)-Fyn couples human oligomeric Aβ with pathological tau changes in Alzheimer's disease. *J. Neurosci.* 32:16857–71a. http://dx.doi.org/10.1523/JNEUROSCI.1858-12.2012

Laurén, J., D.A. Gimbel, H.B. Nygaard, J.W. Gilbert, and S.M. Strittmatter. 2009. Cellular prion protein mediates impairment of synaptic plasticity by amyloid-beta oligomers. *Nature.* 457:1128–1132. http://dx.doi.org/10.1038/nature07761

Legrand, N., N.D. Huntington, M. Nagasawa, A.Q. Bakker, R. Schotte, H. Strick-Marchand, S.J. de Geus, S.M. Pouw, M. Böhne, A. Voordouw, et al. 2011. Functional CD47/signal regulatory protein alpha (SIRP(alpha)) interaction is required for optimal human T- and natural killer- (NK) cell homeostasis in vivo. *Proc. Natl. Acad. Sci. USA.* 108:13224–13229. http://dx.doi.org/10.1073/pnas.1101398108

Li, B., and C.N. Dewey. 2011. RSEM: accurate transcript quantification from RNA-Seq data with or without a reference genome. *BMC Bioinformatics.* 12:323. http://dx.doi.org/10.1186/1471-2105-12-323

Li, L., X. Xiao, S. Li, X. Jia, P. Wang, X. Guo, X. Jiao, Q. Zhang, and J.F. Hejtmancik. 2011. Detection of variants in 15 genes in 87 unrelated Chinese patients with Leber congenital amaurosis. *PLoS ONE.* 6:e19458. http://dx.doi.org/10.1371/journal.pone.0019458

Linden, R., V.R. Martins, M.A. Prado, M. Cammarota, I. Izquierdo, and R.R. Brentani. 2008. Physiology of the prion protein. *Physiol. Rev.* 88:673–728. http://dx.doi.org/10.1152/physrev.00007.2007

Lledo, P.M., P. Tremblay, S.J. DeArmond, S.B. Prusiner, and R.A. Nicoll. 1996. Mice deficient for prion protein exhibit normal neuronal excitability and synaptic transmission in the hippocampus. *Proc. Natl. Acad. Sci. USA.* 93:2403–2407. http://dx.doi.org/10.1073/pnas.93.6.2403

Manson, J.C., A.R. Clarke, M.L. Hooper, L. Aitchison, I. McConnell, and J. Hope. 1994. 129/Ola mice carrying a null mutation in PrP that abolishes mRNA production are developmentally normal. *Mol. Neurobiol.* 8:121–127. http://dx.doi.org/10.1007/BF02780662

Matozaki, T., Y. Murata, H. Okazawa, and H. Ohnishi. 2009. Functions and molecular mechanisms of the CD47-SIRPalpha signalling pathway. *Trends Cell Biol.* 19:72–80. http://dx.doi.org/10.1016/j.tcb.2008.12.001

Moore, R.C., N.J. Redhead, J. Selfridge, J. Hope, J.C. Manson, and D.W. Melton. 1995. Double replacement gene targeting for the production of a series of mouse strains with different prion protein gene alterations. *Biotechnology (N. Y.).* 13:999–1004. http://dx.doi.org/10.1038/nbt0995-999

Ng, P.C., and S. Henikoff. 2001. Predicting deleterious amino acid substitutions. *Genome Res.* 11:863–874. http://dx.doi.org/10.1101/gr.176601

Nico, P.B., F. de-Paris, E.R. Vinadé, O.B. Amaral, I. Rockenbach, B.L. Soares, R. Guarnieri, L. Wichert-Ana, F. Calvo, R. Walz, et al. 2005. Altered behavioural response to acute stress in mice lacking cellular prion protein. *Behav. Brain Res.* 162:173–181. http://dx.doi.org/10.1016/j.bbr.2005.02.003

Nitta, K., A. Sakudo, J. Masuyama, G. Xue, K. Sugiura, and T. Onodera. 2009. Role of cellular prion proteins in the function of macrophages

and dendritic cells. *Protein Pept. Lett.* 16:239–246. http://dx.doi.org/10.2174/092986609787601705

Oh, J.M., H.Y. Shin, S.J. Park, B.H. Kim, J.K. Choi, E.K. Choi, R.I. Carp, and Y.S. Kim. 2008. The involvement of cellular prion protein in the autophagy pathway in neuronal cells. *Mol. Cell. Neurosci.* 39:238–247. http://dx.doi.org/10.1016/j.mcn.2008.07.003

Oh, J.M., E.K. Choi, R.I. Carp, and Y.S. Kim. 2012. Oxidative stress impairs autophagic flux in prion protein–deficient hippocampal cells. *Autophagy*. 8:1448–1461. http://dx.doi.org/10.4161/auto.21164

Ohnishi, H., T. Murata, S. Kusakari, Y. Hayashi, K. Takao, T. Maruyama, Y. Ago, K. Koda, F.J. Jin, K. Okawa, et al. 2010. Stress-evoked tyrosine phosphorylation of signal regulatory protein α regulates behavioral immobility in the forced swim test. *J. Neurosci.* 30:10472–10483. http://dx.doi.org/10.1523/JNEUROSCI.0257-10.2010

Oliferenko, S., K. Paiha, T. Harder, V. Gerke, C. Schwärzler, H. Schwarz, H. Beug, U. Günthert, and L.A. Huber. 1999. Analysis of CD44-containing lipid rafts: Recruitment of annexin II and stabilization by the actin cytoskeleton. *J. Cell Biol.* 146:843–854. http://dx.doi.org/10.1083/jcb.146.4.843

Peyron, P., C. Bordier, E.N. N'Diaye, and I. Maridonneau-Parini. 2000. Nonopsonic phagocytosis of *Mycobacterium kansasii* by human neutrophils depends on cholesterol and is mediated by CR3 associated with glyco-sylphosphatidylinositol-anchored proteins. *J. Immunol.* 165:5186–5191.

Polymenidou, M., R. Moos, M. Scott, C. Sigurdson, Y.Z. Shi, B. Yajima, I. Hafner-Bratkovic, R. Jerala, S. Hornemann, K. Wuthrich, et al. 2008. The POM monoclonals: a comprehensive set of antibodies to non-overlapping prion protein epitopes. *PLoS ONE*. 3:e3872. http://dx.doi.org/10.1371/journal.pone.0003872

Rangel, A., F. Burgaya, R. Gavín, E. Soriano, A. Aguzzi, and J.A. Del Río. 2007. Enhanced susceptibility of Prnp-deficient mice to kainate-induced seizures, neuronal apoptosis, and death: Role of AMPA/kainate receptors. *J. Neurosci. Res.* 85:2741–2755. http://dx.doi.org/10.1002/jnr.21215

Ratté, S., M. Vreugdenhil, J.K. Boult, A. Patel, E.A. Asante, J. Collinge, and J.G. Jefferys. 2011. Threshold for epileptiform activity is elevated in prion knockout mice. *Neuroscience*. 179:56–61. http://dx.doi.org/10.1016/j.neuroscience.2011.01.053

Ridgway, W.M., B. Healy, L.J. Smink, D. Rainbow, and L.S. Wicker. 2007. New tools for defining the 'genetic background' of inbred mouse strains. *Nat. Immunol.* 8:669–673. http://dx.doi.org/10.1038/ni0707-669

Rossi, D., A. Cozzio, E. Flechsig, M.A. Klein, T. Rülicke, A. Aguzzi, and C. Weissmann. 2001. Onset of ataxia and Purkinje cell loss in PrP null mice inversely correlated with Dpl level in brain. *EMBO J.* 20:694–702. http://dx.doi.org/10.1093/emboj/20.4.694

Sakaguchi, S., S. Katamine, K. Shigematsu, A. Nakatani, R. Moriuchi, N. Nishida, K. Kurokawa, R. Nakaoke, H. Sato, K. Jishage, et al. 1995. Accumulation of proteinase K-resistant prion protein (PrP) is restricted by the expression level of normal PrP in mice inoculated with a mouse-adapted strain of the Creutzfeldt-Jakob disease agent. *J. Virol.* 69:7586–7592.

Sano, S., H. Ohnishi, and M. Kubota. 1999. Gene structure of mouse BIT/SHPS-1. *Biochem. J.* 344:667–675. http://dx.doi.org/10.1042/0264-6021:3440667

Scott, R.S., E.J. McMahon, S.M. Pop, E.A. Reap, R. Caricchio, P.L. Cohen, H.S. Earp, and G.K. Matsushima. 2001. Phagocytosis and clearance of apoptotic cells is mediated by MER. *Nature*. 411:207–211. http://dx.doi.org/10.1038/35075603

Seitz, H.M., T.D. Camenisch, G. Lemke, H.S. Earp, and G.K. Matsushima. 2007. Macrophages and dendritic cells use different Axl/Mertk/Tyro3 receptors in clearance of apoptotic cells. *J. Immunol.* 178:5635–5642.

Smithies, O., and N. Maeda. 1995. Gene targeting approaches to complex genetic diseases: atherosclerosis and essential hypertension. *Proc. Natl. Acad. Sci. USA*. 92:5266–5272. http://dx.doi.org/10.1073/pnas.92.12.5266

Sparkes, R.S., M. Simon, V.H. Cohn, R.E. Fournier, J. Lem, I. Klisak, C. Heinzmann, C. Blatt, M. Lucero, T. Mohandas, et al. 1986. Assignment of the human and mouse prion protein genes to homologous chromosomes. *Proc. Natl. Acad. Sci. USA*. 83:7358–7362. http://dx.doi.org/10.1073/pnas.83.19.7358

Steele, A.D., S. Lindquist, and A. Aguzzi. 2007. The prion protein knockout mouse: a phenotype under challenge. *Prion*. 1:83–93. http://dx.doi.org/10.4161/pri.1.2.4346

Striebel, J.F., B. Race, M. Pathmajeyan, A. Rangel, and B. Chesebro. 2013. Lack of influence of prion protein gene expression on kainate-induced seizures in mice: studies using congenic, coisogenic and transgenic strains. *Neuroscience*. 238:11–18. http://dx.doi.org/10.1016/j.neuroscience.2013.02.004

Strom, A., G.S. Wang, and F.W. Scott. 2011. Impaired glucose tolerance in mice lacking cellular prion protein. *Pancreas*. 40:229–232. http://dx.doi.org/10.1097/MPA.0b013e3181f7e547

Strowig, T., A. Rongvaux, C. Rathinam, H. Takizawa, C. Borsotti, W. Philbrick, E.E. Eynon, M.G. Manz, and R.A. Flavell. 2011. Transgenic expression of human signal regulatory protein alpha in Rag2-/-gamma(c)-/- mice improves engraftment of human hematopoietic cells in humanized mice. *Proc. Natl. Acad. Sci. USA*. 108:13218–13223. http://dx.doi.org/10.1073/pnas.1109769108

Takenaka, K., T.K. Prasolava, J.C. Wang, S.M. Mortin-Toth, S. Khalouei, O.I. Gan, J.E. Dick, and J.S. Danska. 2007. Polymorphism in Sirpa modulates engraftment of human hematopoietic stem cells. *Nat. Immunol.* 8:1313–1323. http://dx.doi.org/10.1038/ni1527

Theocharides, A.P., L. Jin, P.Y. Cheng, T.K. Prasolava, A.V. Malko, J.M. Ho, A.G. Poeppl, N. van Rooijen, M.D. Minden, J.S. Danska, et al. 2012. Disruption of SIRPα signaling in macrophages eliminates human acute myeloid leukemia stem cells in xenografts. *J. Exp. Med.* 209:1883–1899. http://dx.doi.org/10.1084/jem.20120502

Tomizawa, T., Y. Kaneko, Y. Kaneko, Y. Saito, H. Ohnishi, J. Okajo, C. Okuzawa, T. Ishikawa-Sekigami, Y. Murata, H. Okazawa, et al. 2007. Resistance to experimental autoimmune encephalomyelitis and impaired T cell priming by dendritic cells in Src homology 2 domain-containing protein tyrosine phosphatase substrate-1 mutant mice. *J. Immunol.* 179:869–877.

Tsutsui, S., J.N. Hahn, T.A. Johnson, Z. Ali, and F.R. Jirik. 2008. Absence of the cellular prion protein exacerbates and prolongs neuroinflammation in experimental autoimmune encephalomyelitis. *Am. J. Pathol.* 173:1029–1041. http://dx.doi.org/10.2353/ajpath.2008.071062

Um, J.W., H.B. Nygaard, J.K. Heiss, M.A. Kostylev, M. Stagi, A. Vortmeyer, T. Wisniewski, E.C. Gunther, and S.M. Strittmatter. 2012. Alzheimer amyloid-β oligomer bound to postsynaptic prion protein activates Fyn to impair neurons. *Nat. Neurosci.* 15:1227–1235. http://dx.doi.org/10.1038/nn.3178

Uraki, R., A. Sakudo, S. Ando, H. Kitani, and T. Onodera. 2010. Enhancement of phagocytotic activity by prion protein in PrP-deficient macrophage cells. *Int. J. Mol. Med.* 26:527–532.

Walz, R., O.B. Amaral, I.C. Rockenbach, R. Roesler, I. Izquierdo, E.A. Cavalheiro, V.R. Martins, and R.R. Brentani. 1999. Increased sensitivity to seizures in mice lacking cellular prion protein. *Epilepsia*. 40:1679–1682. http://dx.doi.org/10.1111/j.1528-1157.1999.tb01583.x

Wolfer, D.P., W.E. Crusio, and H.P. Lipp. 2002. Knockout mice: simple solutions to the problems of genetic background and flanking genes. *Trends Neurosci.* 25:336–340. http://dx.doi.org/10.1016/S0166-2236(02)02192-6

Yamauchi, T., K. Takenaka, S. Urata, T. Shima, Y. Kikushige, T. Tokuyama, C. Iwamoto, M. Nishihara, H. Iwasaki, T. Miyamoto, et al. 2013. Polymorphic Sirpa is the genetic determinant for NOD-based mouse lines to achieve efficient human cell engraftment. *Blood*. 121:1316–1325. http://dx.doi.org/10.1182/blood-2012-06-440354

Yokoyama, T., K.M. Kimura, Y. Ushiki, S. Yamada, A. Morooka, T. Nakashiba, T. Sassa, and S. Itohara. 2001. In vivo conversion of cellular prion protein to pathogenic isoforms, as monitored by conformation-specific antibodies. *J. Biol. Chem.* 276:11265–11271. http://dx.doi.org/10.1074/jbc.M008734200